Vol 18 No 6, June 2009
1674-1056/2009/18(06)/2603-07

Chinese Physics B

© 2009 Chin. Phys. Soc.
and IOP Publishing Ltd

Strain effects on the polarized optical properties of InGaN with different In compositions*

Tao Ren-Chun(陶仁春), Yu Tong-Jun(于彤军)†, Jia Chuan-Yu(贾传宇),
Chen Zhi-Zhong(陈志忠), Qin Zhi-Xin (秦志新), and Zhang Guo-Yi(张国义)

State Key Laboratory for Mesoscopic Physics, School of Physics, Peking University, Beijing 100871, *China*

(Received 11 November 2008; revised manuscript received 22 December 2008)

Strain effects on the polarized optical properties of c-plane and m-plane $In_xGa_{1-x}N$ were discussed for different In compositions ($x = 0$, 0.05, 0.10, 0.15) by analyzing the relative oscillator strength (ROS) and energy level splitting of the three transitions related to the top three valence bands (VBs). The ROS was calculated by applying the effective-mass Hamiltonian based on $\boldsymbol{k}\cdot\boldsymbol{p}$ perturbation theory. For c-plane $In_xGa_{1-x}N$, it was found that the ROS of $|X\rangle$ and $|Y\rangle$-like states were superposed with each other. Especially, under compressive strain, they dominated in the top VB whose energy level also went up with strain, while the ROS of the $|Z\rangle$-like state decreased in the second band. For m-plane $In_xGa_{1-x}N$ under compressive strain, the top three VBs were dominated by $|X\rangle$, $|Z\rangle$, and $|Y\rangle$-like states, respectively, which led to nearly linearly-polarized light emissions. For the top VB, ROS difference between $|X\rangle$ and $|Z\rangle$-like states became larger with compressive strain. It was also found that such tendencies were more evident in layers with higher In compositions. As a result, there would be more TE modes in total emissions from both c-plane and m-plane InGaN with compressive strain and In content, leading to a larger polarization degree. Experimental results of luminescence from InGaN/GaN quantum wells (QWs) showed good coincidence with our calculations.

Keywords: GaN, polarization degree, m-plane, relative oscillator strength
PACC: 7840F, 4225J, 3720C

1. Introduction

Wurzite (WZ) gallium nitride (GaN) and related alloys have received enormous attention because of their broad range of practical applications. Among the ternary compounds of III-nitride materials, InGaN has been considered as the most important and indispensable material for the fabrication of light emitters which are active in entire visible and part of near-UV spectral regions. The optical properties of InGaN have been intensively studied during the last decade. One of the most interesting research directions is on the polarization property of InGaN material.[1]

The polarized optical phenomenon of GaN was first observed by Dingle *et al* in 1971.[2] Previous studies centered on c-plane GaN-based materials,[3−5] while current research focuses on nonpolar and semipolar materials.[6−10] Studying polarized optical property can help enhance the light extraction of light emitting diodes (LEDs) and lasers.[11] What is more important, devices, such as LEDs, with polarized emissions, have many applications, including liquid crystal display (LCD) back lighting[1] and image processing.[12] Because of its vast potential applications, controlling the polarized optical property of InGaN becomes an important issue.

It is well known that strain universally exists in devices with InGaN as an active layer due to lattice mismatch and difference in thermal expansion coefficiencies between the epilayer and the substrate. It has been established that strain can modify the electronic band structures of WZ GaN[13]. Moreover, besides the lattice constant, many other material parameters of InN are remarkably different with those of GaN: for example, band gap, elastic constants, effective electron mass and so on. As a result, samples with different In compositions would also have different electronic band structures, which should also correspond to different polarized optical property. It is expected that adjusting strain and In content can be a way to control the polarized optical properties of InGaN. The luminescence mode of c-plane GaN/AlGaN QW under biaxial strain has been studied theoretically,[14] and the polarized optical absorption property of GaN

*Project supported by the National Natural Science Foundation of China (Grant Nos 60676032, 60577030 and 60776042) and National Key Basic Research Special Foundation of China (Grant No TG 2007CB307004).
†Corresponding author. E-mail: tongjun@pku.edu.cn

varying with strain was analyzed by Ghosh *et al.*[15] Gil *et al* have done lots of basic work on the optical anisotropy of GaN varying with different strains.[16,17] However, reports on the polarized optical emission property of InGaN varying with different strains are still lacking. Whereas, these works provide good examples to perform theoretical analysis of strain's effects on the polarized optical property of InGaN with different In content using the Hamiltonian matrix for wurtzite structure materials based on the $\boldsymbol{k}\cdot\boldsymbol{p}$ method.

Recent advances in crystal growth techniques enable the fabrication of high-quality InGaN devices on substrates with orientations other than the conventional [0001] direction.[18] These nonpolar or semipolar divices are believed to eliminate piezoelectric polarization and partly reduce spontaneous polarization and have an improved device quality. The M-plane device can be a representative of them. But the traditional c-plane materials are still widely applied in laboratory and industry for their good crystal quality. Therefore, in this paper, stain's influence on the polarized optical property is discussed for c-plane and m-plane InGaN. The theoretical calculation is based on $\boldsymbol{k}\cdot\boldsymbol{p}$ perturbation theory. We discuss the physical origin of the polarized light emission of InGaN in terms of VB splitting and the components of interband transition's ROS of the top three VBs. Experimentally, the polarization degrees of spontaneous edge emitting electro-luminescence (EL) of near-UV LEDs InGaN/GaN grown on (0001) sapphire were also measured. The experimental results supported our theoretical analyses well.

2. Theoretical calculation

A 3×3 Hamiltonian (at $\Gamma = 0$)[19] for WZ GaN obtained from a 6×6 one has been applied:[20]

$$H = \begin{bmatrix} F & K & -\mathrm{i}H \\ K & G & \Delta - \mathrm{i}H \\ \mathrm{i}H & \Delta + \mathrm{i}H & \lambda \end{bmatrix} \tag{1}$$

with its three basic vectors

$$\begin{aligned} |1\rangle &= \alpha^* |U_1\rangle + \alpha |U_4\rangle , \\ |2\rangle &= \beta |U_2\rangle + \beta^* |U_5\rangle , \\ |3\rangle &= \beta^* |U_3\rangle + \beta |U_6\rangle , \end{aligned} \tag{2}$$

where

$$\alpha = \frac{1}{\sqrt{2}} \mathrm{e}^{\mathrm{i}(3\pi/4)}, \quad \beta = \frac{1}{\sqrt{2}} \mathrm{e}^{\mathrm{i}(\pi/4)} \tag{3}$$

and

$$\begin{aligned} |U_1\rangle &= -\frac{1}{\sqrt{2}} |(X + \mathrm{i}Y) \uparrow\rangle , \\ |U_2\rangle &= \frac{1}{\sqrt{2}} |(X - \mathrm{i}Y) \uparrow\rangle , \\ |U_3\rangle &= |Z \uparrow\rangle , \\ |U_4\rangle &= \frac{1}{\sqrt{2}} |(X - \mathrm{i}Y) \downarrow\rangle , \\ |U_5\rangle &= -\frac{1}{\sqrt{2}} |(X + \mathrm{i}Y) \downarrow\rangle , \\ |U_6\rangle &= |Z \downarrow\rangle . \end{aligned} \tag{4}$$

The abbreviations used in matrix (1) and Eq.(3) are

$$\begin{aligned} F &= \Delta_1 + \Delta_2 + \lambda + \theta, \\ G &= \Delta_1 - \Delta_2 + \lambda + \theta, \\ K &= D_5 \varepsilon_+, \\ H &= D_6 \varepsilon_{z+}, \\ \Delta &= \sqrt{2} \Delta_3, \\ \lambda &= \lambda_\varepsilon, \\ \theta &= \theta_\varepsilon, \end{aligned} \tag{5}$$

where

$$\begin{aligned} \lambda_\varepsilon &= D_1 \varepsilon_{zz} + D_2 (\varepsilon_{xx} + \varepsilon_{yy}), \\ \theta_\varepsilon &= D_3 \varepsilon_{zz} + D_4 (\varepsilon_{xx} + \varepsilon_{yy}), \\ \varepsilon_\pm &= \varepsilon_{xx} \pm 2\mathrm{i}\varepsilon_{xy} - \varepsilon_{yy}, \\ \varepsilon_{z\pm} &= \varepsilon_{zx} \pm \mathrm{i}\varepsilon_{yz}. \end{aligned} \tag{6}$$

The parameters D_i's (i = 1 to 6) denote deformation potentials for VBs and ε_{ij} are components of the strain tensor. Δ_1 is the crystal-field energy parameter, while Δ_2 and Δ_3 are spin-orbit energy parameters. For different In compositions, all these parameters of $\mathrm{In}_x\mathrm{Ga}_{1-x}\mathrm{N}$ are linearly interpolated between those of GaN and InN.

The coordinate system in our calculation is described in Fig.1. The z axis corresponds to the c axis [0001], and x is along $[11\bar{2}0]$ with y along $[1\bar{1}00]$.

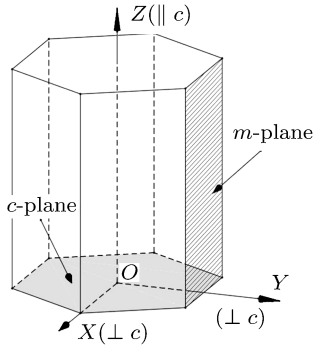


Fig.1. The coordinate system in our calculation.

For c-plane $In_xGa_{1-x}N$ grown on GaN or sapphire, the strain existing in the x–y plane is compressively biaxial. Consequently, the biaxial strain mode is employed in our calculation for c-plane InGaN. In addition, the calculation also includes cases under tensile strain.

The strain tensors for the c-plane $In_xGa_{1-x}N$ calculation comprise of

$$\begin{aligned} \varepsilon_{xx} &= \varepsilon_{yy}, \\ \varepsilon_{zz} &= -\frac{2C_{13}}{C_{33}}\varepsilon_{xx}, \\ \varepsilon_{xy} &= \varepsilon_{xz} = \varepsilon_{yz} = 0, \end{aligned} \tag{7}$$

where C_{ij}'s are stiffness constants.

The wave functions of VBs, which are obtained by solving equation

$$H^U |\Psi^{vb}\rangle = E |\Psi^{vb}\rangle, \tag{8}$$

can be described as

$$\left|\Psi^{vb}\right\rangle = a\,|X\rangle + b\,|Y\rangle + c\,|Z\rangle\,, \tag{9}$$

where coefficients, a, b and c, are obtained from eigenvectors of H^U. The emission modes are determined by the momentum matrix elements, $M_{nm,l}(k) = \langle \Psi^v_{m,k}|p_l|\Psi^c_{n,k}\rangle$, with $l = x, y, z$. In our calculation, $|\Psi^c_n\rangle = |S\rangle$, and $|X\rangle$, $|Y\rangle$, $|Z\rangle$ and $|S\rangle$ are the p_x, p_y, p_z and s orbital wave functions, respectively. $|X\rangle$-like and $|Y\rangle$-like states contribute to transverse electric (TE) mode light emission with its polarization $\boldsymbol{E} \perp \boldsymbol{c}$. $|Z\rangle$-like states contribute to transverse magnetic (TM) mode light emission with its polarization $\boldsymbol{E} \parallel \boldsymbol{c}$. According to earlier theoretical results, $|\langle S|\,p_x\,|X\rangle|^2$, $|\langle S|\,p_y\,|Y\rangle|^2$, and $|\langle S|\,p_z\,|Z\rangle|^2$ can be taken as equal.[21] Therefore, the relative components of $|X\rangle$-like, $|Y\rangle$-like and $|Z\rangle$-like states in wave functions can represent the ROS of transitions. Generally, the ROS expresses the strength of transitions, directly relating to the recombination of electrons in the conduction band and holes in VBs.

The strain situation is expected to be quite different for m-plane InGaN. While biaxial in-plane (x–y plane) strain in the c-plane sample can preserve the original symmetry of wurtzite structures, the in-plane (x–z plane) strain in m-plane InGaN would reduce the C_{6v} symmetry to C_{2v}. The strain components relations can be written as follows.[22]

$$\begin{aligned} \varepsilon_{yy} &= -\frac{C_{12}+C_{13}}{C_{11}}\varepsilon_{zz}, \\ \varepsilon_{xy} &= \varepsilon_{yz} = \varepsilon_{zx} = 0, \end{aligned} \tag{10}$$

which is biaxial ($\varepsilon_{xx} = \varepsilon_{zz}$). It is believed that the change of optical polarization is closely related with the symmetry in the basal plane (x–y plane) of the wurtzite structure. Strain in the m-plane induces the symmetry break in the basal plane (x–y plane). A biaxial in-plane (x–z plane) strain of m-plane samples is simple, but provides the convenience of simplifying the calculation and analyses of results.

3. Results and discussion

With parameters recommended by Vurgaftman and Meyer[23] (in Table 1), VB energy level splitting and the ROS of transitions at the Γ point are calculated for InGaN with different In compositions.

Table 1. Parameters for GaN and InN.

Parameters	GaN	InN
Δ_{cr}=Δ_1/eV	0.010	0.040
Δ_{so}=3Δ_2=3Δ_3/eV	0.017	0.005
D_1/eV	–3.7	–3.7
D_2/eV	4.5	4.5
D_3/eV	8.2	8.2
D_4/eV	–4.1	–4.1
D_5/eV	–4.0	–4.0
D_6/eV	–5.5	–5.5
C_{11}/GPa	390	223
C_{12}/GPa	145	115
C_{13}/GPa	106	92
C_{33}/GPa	398	224

Figures 2 and 3 are the calculation results of the ROS and energy levels of c-plane $In_xGa_{1-x}N$, which are presented as functions of strain. From Fig.2, it can be clearly seen that, for any In compositions, the ROS of $|X\rangle$ and $|Y\rangle$-like states are the same in all the top three VBs. They superpose with each other at any given ε_{yy}, presenting the nature that the biaxial in-plane (x–y plane) strain in c-plane InGaN preserves the original symmetry of the wurtzite structure.

Under compressive strain, the ROS of the three VBs changes differently. For c-plane samples with any In content, there is no ROS of the $|Z\rangle$-like state and that of the $|X\rangle$ and $|Y\rangle$-like states does not change with strain in the top VB. However, with respect to the second VB, the ROS of the $|Z\rangle$-like state decreases with increasing compressive strain while ROS of the $|X\rangle$ and $|Y\rangle$-like states increases. Although

the ROS of the $|Z\rangle$-like state increases with increasing compressive strain and dominates the third VB under large strain [Fig.2(c)], the energy level of the third VB drops remarkably in Fig.3. On the other hand, the top and the second energy levels go up. As a result, TE modes contributed by the $|X\rangle$- and $|Y\rangle$-like states, which dominate in the top two VBs, increase while TM modes contributed by the $|Z\rangle$-like state would decrease.

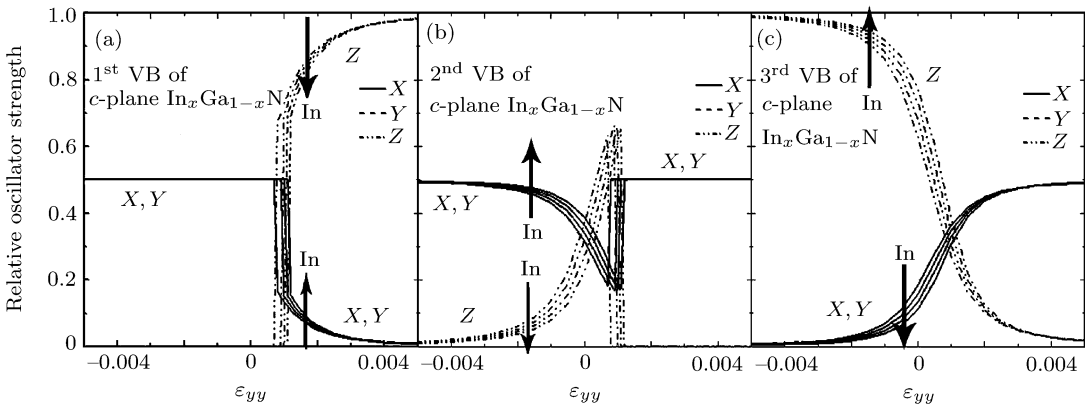


Fig.2. ROS of VBs of c-plane InGaN as functions of strain ($x = 0$, 0.05, 0.10, 0.15).

Moreover, in samples with different In contents ($x = 0$, 0.05, 0.10, 0.15), strain's effects on the ROS and energy levels of VBs also change. From Fig.2, it can be seen that, when $\varepsilon_{yy} < 0$, that is, the strain is compressive, no ROS variation occurs for the top VB with increasing In content. Whereas, The ROS of the $|Z\rangle$-like state decreases in the second band and increases in the third one and that of the $|X\rangle$- and $|Y\rangle$-like states changes reversely. But the mode contribution of the third band is small for its much lower energy level as mentioned above. The reinforce effect of the ROS of the $|Z\rangle$-like state in the third VB with increasing In content could also be neglected. Further, as shown in Fig.3, for samples with more In content, the energy levels of the top and the second VBs also increase more rapidly with compressive strain. All these changes related to increasing In content are favorable factors that would enhance TE mode light emission and inhibit TM mode light emission from c-plane InGaN. If the in-plane biaxial strain in c-plane InGaN becomes larger and larger and at the same time In content also increases, the polarization degree,

$$P = \frac{I_{\mathrm{TE}} - I_{\mathrm{TM}}}{I_{\mathrm{TE}} + I_{\mathrm{TM}}}, \tag{11}$$

would increase accordingly. Here I_{TE} and I_{TM} are the light emission intensity of TE mode and TM mode, respectively.

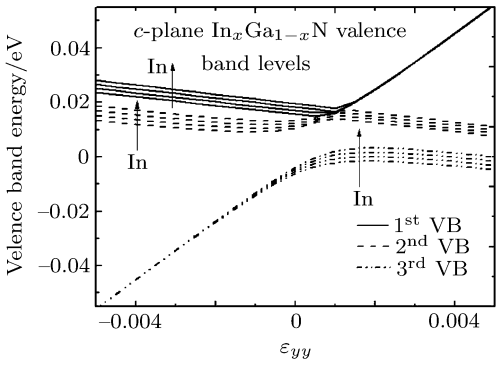


Fig.3. VB energy splitting of c-plane $In_xGa_{1-x}N$ as functions of strain ($x = 0$, 0.05, 0.10, 0.15).

In addition, under tensile strain ($\varepsilon_{yy} > 0$ for c-plane InGaN, or $\varepsilon_{zz} > 0$ for the m-plane InGaN), the ROS and energy band structure change very differently from those of InGaN layers under compressive strain, as shown in Fig.2 and Fig.3. From Fig.2(a), it can be seen that the top VB is dominated by the $|Z\rangle$-like state and the ROS contributed by the $|Z\rangle$-like states increases with increasing tensile strain. As for the energy level of $In_xGa_{1-x}N$, the topmost VB dominated by the $|Z\rangle$-like state goes up sharply with increasing tensile strain, but the other two bands go

down. Emissions dominated by the z-polarized TM light would come out, and the more TM mode emission with larger tensile strain.

The calculation of the ROS and the splitting of VBs at the Γ point is also performed for m-plane $In_xGa_{1-x}N$. From Fig.4, it can be seen that the ROS of the $|X\rangle$-like and $|Y\rangle$-like states in every VB do not superpose with each other, which is different from those in the c-plane. This is because the x–z plane strain in m-plane samples induces symmetry breaking in the x–y plane, turning C_{6v} symmetry into C_{2v} symmetry, so as to change the VB wave functions. The third VB contributes little to the total light emission modes because of its lower energy level. The top two VBs are mainly discussed. As shown in Fig.4, for m-plane $In_xGa_{1-x}N$ samples under compressive strain ($\varepsilon_{zz} < 0$), the ROS of the $|X\rangle$-like state in the first VB, the ROS of the $|Z\rangle$-like state in the second one and the $|Y\rangle$-like state in the third one, all increase with compressive strain. The TM mode light emission, which is contributed by the ROS of the $|Z\rangle$-like states, mainly comes from the second VB. But the ROS of the $|X\rangle$-like states in the top VB, which contributes to the x-polarized TE mode light emission, increases more rapidly than that of the $|Z\rangle$-like states in the second one. This is beneficial to x-polarized TE mode light emission. And from Fig.5, it can be seen that the energy level of the top VB goes up a little more dramatically than the second one. This would favor the light emission of the first VB, which contributes mostly to x-polarized TE mode light emission. Therefore, there would be more x-polarized TE mode light emission and less z-polarized TM mode light emission from m-plane $In_xGa_{1-x}N$ with increasing compressive strain. It means an increasing polarization degree. Besides, when the compressive strain is large enough, $|X\rangle$, $|Z\rangle$, and $|Y\rangle$-like states dominate the first, the second and the third VBs, respectively. Consequently, nearly linearly-polarized light emission would come out.

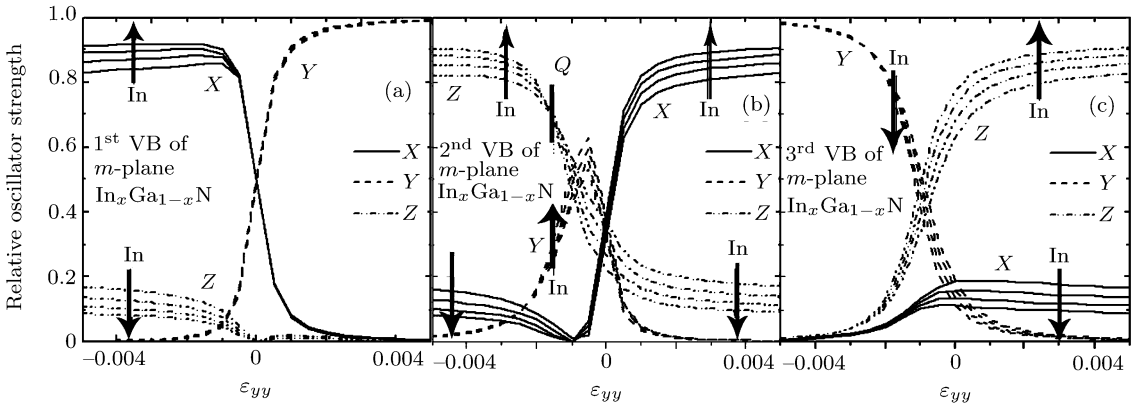


Fig.4. The ROS of m-plane InGaN as functions of strain for different In compositions (x = 0, 0.05, 0.10, 0.15).

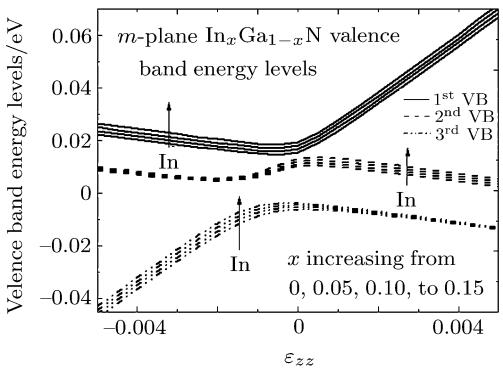


Fig.5. VB energy level splitting in m-plane $In_xGa_{1-x}N$ as functions of strain.

As shown in Fig.4(a), it can be seen that, for $In_xGa_{1-x}N$ with more In composition, the ROS of the $|X\rangle$-like state in the top VB increases more remarkably with compressive strain, while for that of the $|Z\rangle$-like state, the strain's effect becomes less significant. The ROS of the $|Z\rangle$-like state in the second VB increases with In compositions at first when the compressive strain is not very large (on the right side of line Q in Fig.4(b)), and increases when the strain is raised to a certain amount (on the left side of line Q in Fig.4(b)). However, the energy level of the top VB goes up with In composition in Fig.5. With in-

creasing In content, the up-going of the energy level and the ROS of the $|X\rangle$-like state of the first band and the decreasing of the ROS of the $|Z\rangle$-like state, are all favorable factors that would enhance x-polarized TE mode emission.

Therefore, if the strain and In content of m-plane samples can be raised at the same time, there would be more x-polarized TE mode emission and less z-polarized TM mode emission, resulting in greater polarization. The cases under tensile strain ($\varepsilon_{zz} > 0$) are also considered for m-plane InGaN. As shown in Fig.4(a)–4(c), the top three VBs are dominated by $|Y\rangle$, $|X\rangle$, $|Z\rangle$-like states, respectively. It is distinct from cases under compressive strain. The energy levels of the second and the third VBs, from which z-polarized TM mode light is mainly emitted out, decrease with tensile strain. TE mode light emission mostly comes from the ROS of the $|Y\rangle$-like states of the top VB whose energy level goes up with tensile strain. Therefore, there might be a much larger polarization degree compared with the cases under compressive strain.

4. Experiments

These strain effects on the polarized optical properties of $In_xGa_{1-x}N$ with different In compositions can be observed experimentally from the luminescence of $In_xGa_{1-x}N$ devices.

It is considered that in-plane strains both in multiple quantum wells (MQWs) and bulk $In_xGa_{1-x}N$ give similar effects on lattice symmetry, and can be more easily observed in MQWs because of their stronger light emissions. The LEDs used in our experiment were grown on (0001) sapphire by metal organic chemical vapor deposition (MOCVD). These devices consisted of Si-doped GaN, several periods of InGaN/GaN (3 nm/10 nm) MQWs, and Mg-doped GaN. The indium compositions in InGaN well layers of these samples were different. The chip size was 300 $\mu m \times 300$ μm. The experimental setup has been illustrated elsewhere.[24] From the polarized EL spectrum, the polarization degree can be obtained.

Figure 6(a) shows the polarization degree as a function of light wavelength for c-plane InGaN/GaN MQWs. It is found that longer wavelength emissions are stronger polarized. It is known that the more indium in the wells, the larger the compressive strain, and the longer the wavelength. In other words, the polarization degree of InGaN/GaN MQWs increases with compressive strain and In contents. The similar photoluminescence (PL) results (Fig.6(b)) could also be found for m-plane InGaN/GaN MQWs.[25] Obviously, these experimental results from c-plane and m-plane InGaN support the theoretical analyses well. It suggests that adjusting the strain and In composition can be a feasible way to control the polarized optical properties of InGaN.

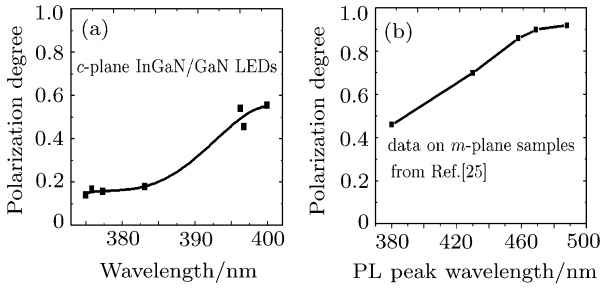


Fig.6. (a) Polarization degree of edge-emitted EL from near UV-LEDs increases as a function of wavelength from 375 nm to 400 nm. (b) The polarization degree as a function of PL peak wavelength for m-plane InGaN.

5. Conlusions

In summary, a Hamiltonian based on $\boldsymbol{k}\cdot\boldsymbol{p}$ perturbation theory was applied to calculate the energy splitting and the ROS of the top three VBs at the Γ point. The calculations were performed for c-plane and m-plane InGaN. By analyzing the calculation results, it was deduced that, because of ROS variation and VB energy level splitting, the polarization degree would increase with compressive strain both in c-plane and m-plane $In_xGa_{1-x}N$. For samples with larger In compositions, this tendency with strain would be more evident. The experimental results of polarization of luminescences from InGaN/GaN MQWs supported our calculations well. Finally, it was suggested that adjusting strain and In content is a useful way to control the polarized optical properties of InGaN.

References

[1] Schubert E F and Kim J K 2005 *Science* **308** 1274

[2] Dingle R, Sell D D, Stokowski S E and Ilegems M 1971 *Phys. Rev.* B **4** 1211

[3] Shubina T V, Paskova T, Toropov A A, Ivanov S V and Monemar B 2002 *Phys. Rev.* B **65** 075212

[4] Florescu D I, Lee D S, Ting S M, Ramer J C and Armour

E A 2003 *J. Electron. Mater.* **32** 1330
[5] Nam K B, Li J, Nakarmi M L,Lin J Y and Jiang H X 2004 *Appl. Phys. Lett.* **84** 5264
[6] Gardner N F, Kim J C, Wierer J J, Shen Y C and Krames M R 2005 *Appl. Phys. Lett.* **86** 111101
[7] Masui H, Yamada H, Iso K, Nakamura S and DenBaars S P 2008 *Appl. Phys. Lett.* **92** 091105
[8] Bhattacharyya J, Ghosh S, Arora B M, Brandt O, and Grahn H T 2007 *Appl. Phys. Lett.* **91** 251913
[9] Feneberg M, Lipski F, Sauer R, Thonke K, Brückner P, Neubert B, Wunderer T and Scholz F 2007 *J. Appl. Phys.* **101** 053530
[10] Zou J, Liu C X, Zhou S M, Wang J, Zhou J H, Huang T H, Han P, Xie Z Z and Zhang R 2006 *Chin. Phys.* **15** 2706
[11] Bhattacharyya J, Ghosh S and Grahn H T 2008 *Appl. Phys. Lett.* **93** 051913
[12] Lin S S, Yemelyanov K M, Pugh E N(Jr) and Engheta N 2006 *Opt. Express* **14** 7099
[13] Romanov A E, Waltereit P and Speck J S 2005 *J. Appl. Phys.* **97** 043708
[14] Yeo Y C, Chong T C, Li M F and Fan W J 1998 *IEEE J. Quantum Electron.* **34** 526
[15] Ghosh S, Waltereit P, Brandt O, Grahn H T and Ploog K H 2002 *Phys. Rev.* B **65** 075202
[16] Gil B 1996 *Phys. Rev.* B **54** 7678
[17] Gil B and Alemu A 1997 *Phys. Rev.* B **56** 12446
[18] Kim K C, Schmidt M C, Sato H, Wu F, Fellows N, Saito M, Fujito K, Speck J S, Nakamura S and DenBaars S P 2007 *Phys. Stat. Sol. (RRL)* **1** 125
[19] Park S H and Chuang S L 1999 *Phys. Rev.* B **59** 4725
[20] Chuang S L and Chang C S 1996 *Phys. Rev.* B **54** 2491
[21] Chuang S L 1996 *IEEE J. Quantum Electron.* **32** 1791
[22] Romanov A E, Baker T J, Nakamura S and Speck J S 2006 *J. Appl. Phys.* **100** 023522
[23] Vurgaftman I and Meyer J R 2003 *J. Appl. Phys.* **94** 3675
[24] Jia C Y, Yu T J, Mu S, Pan Y B, Yang Z J, Chen Z Z, Qin Z X and Zhang G Y 2007 *Appl. Phys. Lett.* **90** 211112
[25] Kubota M, Okamoto K, Tanaka T and Ohta H 2008 *Appl. Phys. Lett.* **92** 011920